

# The evolution of the stellar hosts of radio galaxies

Mark Lacy

*Institute of Geophysics and Planetary Physics, L-413 Lawrence Livermore National Laboratory, Livermore CA 94550, and Dept. of Physics, University of California, 1 Shields Avenue, Davis CA 95616*

[mlacy@igpp.ucdavis.edu](mailto:mlacy@igpp.ucdavis.edu)

Andrew J. Bunker <sup>1</sup>

*Department of Astronomy, University of California at Berkeley,  
601 Campbell Hall, Berkeley CA 94720, USA*

[bunker@ast.cam.ac.uk](mailto:bunker@ast.cam.ac.uk)

and

Susan E. Ridgway

*Bloomberg Center for Physics and Astronomy, Johns Hopkins University, 3400 N. Charles Street,  
Baltimore, MD21218*

[ridgway@pha.jhu.edu](mailto:ridgway@pha.jhu.edu)

## ABSTRACT

We present new near-infrared images of  $z > 0.8$  radio galaxies from the flux-limited 7C-III sample of radio sources for which we have recently obtained almost complete spectroscopic redshifts. The 7C objects have radio luminosities  $\approx 20$  times fainter than 3C radio galaxies at a given redshift. The absolute magnitudes of the underlying host galaxies and their scale sizes are only weakly dependent on radio luminosity. Radio galaxy hosts at  $z \sim 2$  are significantly brighter than the hosts of radio-quiet quasars at similar redshifts and the model AGN hosts of Kauffmann & Haehnelt (2000). There is no evidence for strong evolution in scale size, which shows a large scatter at all redshifts. The hosts brighten significantly with redshift, consistent with the passive evolution of a stellar population that formed at  $z \gtrsim 3$ . This scenario is consistent with studies of host galaxy morphology and submillimeter continuum emission, both of which show strong evolution at  $z \gtrsim 2.5$ . The lack of a strong “redshift cutoff” in the radio luminosity function to  $z > 4$  suggests that the formation epoch of the radio galaxy host population lasts  $\gtrsim 1$  Gyr from  $z \gtrsim 5$  to  $z \sim 3$ . We suggest these facts are best explained by models in which the most massive galaxies and their associated AGN form early due to high baryon densities in the centres of their dark matter haloes.

*Subject headings:* galaxies: evolution – galaxies: active – galaxies: formation

## 1. Introduction

At low redshifts, FRI and FRII radio sources with radio luminosities at 151 MHz of  $L_{R(151)} \gtrsim$

$10^{24} \text{WHz}^{-1}$  are associated almost exclusively with giant elliptical host galaxies. If this continues to be the case out to high redshift, then radio galaxies can give us a unique insight into the formation and evolution of a single class of massive galaxy. This is particularly exciting in the light

<sup>1</sup>Current address: Institute of Astronomy, Madingley Road, Cambridge, CB3 OHA, UK

of submillimetre detections of  $z \sim 4$  radio galaxies (e.g. Archibald et al. 2000) which may indicate that we can see these objects during their major bursts of star formation [although see also Willott, Rawlings & Jarvis (2000)]. Furthermore, the similarity of radio galaxy hosts, in contrast to the wide range in luminosity of radio-quiet quasar hosts (McLure et al. 1999; Ridgway et al. 2000), suggests that one of the conditions necessary for producing powerful radio jets is the presence of a massive spheroidal component, and therefore a supermassive ( $\gtrsim 10^9 M_\odot$ ) black hole (Lacy, Ridgway & Trentham 2000).

Studies of high redshift radio galaxy hosts have traditionally concentrated on the  $K - z$  Hubble Diagram. Work on the 3C and 1 Jy samples by Lilly (1989 and refs. therein) initially pointed to a passively-evolving stellar host formed at high redshift which evolved into the giant elliptical radio galaxy hosts seen today, but this was challenged when some high redshift radio galaxies were found to have significant emission line contributions to their  $K$ -band light (Eales & Rawlings 1993, 1996). Only by finding low AGN-luminosity radio galaxies at high redshift could the controversy be resolved. Eales et al. (1997) used the 6C sample, a factor of five fainter in radio flux than the 3C sample, to show that there did seem to be a radio luminosity dependence of host galaxy magnitude. Further work by Roche, Eales & Rawlings (1998) indicated that the hosts of 6C radio galaxies were not only significantly fainter than their 3C counterparts, but also had smaller scale sizes.

We have used the 7C-III radio galaxy redshift survey of Lacy et al. (1999b) to select a complete sample of  $z > 0.8$  radio galaxies. The 7C redshift surveys are a factor of 4–5 lower still in luminosity at a given redshift than the 6C sample of Eales et al. (1997), and thus allow the study of high redshift radio galaxy hosts over a wide range in radio luminosity (Willott et al. 1999). The 7C-III sources were imaged in the near-infrared on the 3-m NASA Infrared Telescope Facility (IRTF) and the 3-m Shane Telescope at Lick Observatory. These data have allowed us to further investigate the radio luminosity dependence of host properties at  $z \sim 1$  and, because our 7C objects at  $z \sim 2$  have similar radio luminosities to  $z \sim 1$  6C radio galaxies and  $z \sim 0.3$  3C radio galaxies, we can also investigate host galaxy evolution over a wide range in

redshift.

We assume a cosmology with  $\Omega_M = 1, \Omega_\Lambda = 0$  and  $H_0 = 50 \text{ km s}^{-1} \text{ Mpc}^{-1}$  except where otherwise stated.

## 2. Observations

Most sources were observed on the IRTF with NSFCAM, a near infrared imaging camera employing a  $256 \times 256$  InSb array, on the nights of 1999 July 28 – 29 UT. The 0.3 arcsec/pixel scale was used for all observations. Details of the observations are given in Table 1. One of the  $J$ ,  $H$  or  $K'$  filters was chosen for each object so as to cover as far as possible the rest-frame  $R$ -band, thus minimizing the  $k$ -correction and the associated uncertainties. In practice this meant that objects with  $0.8 < z < 1.2$  were observed in  $J$ -band, those with  $1.2 < z < 1.8$  in  $H$ -band and those with  $z > 1.8$  in  $K$ -band (using a  $K'$  filter). Exceptions to this were two objects with uncertain redshifts, 7C 1756+6520 and 7C 1804+6313, which were both observed in  $K'$  for ease of estimating photometric redshifts. The sky was clear throughout the run, and most objects were observed in conditions of sub-arcsecond seeing. Two more objects with uncertain redshifts were observed using the Gemini instrument (McLean et al. 1993, 1994) on the Shane Telescope at Lick Observatory on the nights of 1999 June 1 and 4 UT. Gemini was used with a dichroic beamsplitter which enabled us to image in  $J$  and  $K'$  simultaneously. The detector on the short wavelength arm was a  $256 \times 256$  HgCdTe array, and that on the long wavelength arm a  $256 \times 256$  InSb array. The image scale in both arms was 0.68 arcsec/pixel. 7C 1814+6704 was observed in both runs, but the better seeing of the IRTF data allowed more accurate photometry in the moderately crowded field so only the IRTF data is presented. In addition a  $K'$  image of 7C 1745+6624 was presented in Lacy et al. (1999b).

The data were reduced using the DIMSUM package in IRAF, and flat-fielded using dome flats. The final images were magnified by a factor of two before combination to improve the sampling of the final image. The reduced images are shown in Fig. 1 and the photometric properties detailed in Table 2.

TABLE 1  
OBSERVING LOG

Object	Telescope	<i>z</i>	Filter	<i>t</i> <sub>int</sub> /min	FWHM PSF/''
7C 1733+6719	IRTF	1.84	<i>K'</i>	18	0.95
7C 1740+6640	IRTF	2.10	<i>K'</i>	18	0.65
7C 1741+6704	IRTF	1.05	<i>J</i>	13.5	0.65
7C 1742+6346	IRTF	1.27	<i>H</i>	18	0.90
7C 1748+6703	Shane	?	<i>J</i> & <i>K'</i>	56	1.3
7C 1748+6657	IRTF	1.05	<i>J</i>	13.5	0.90
7C 1751+6809	IRTF	1.54	<i>H</i>	18	0.56
7C 1753+6311	Shane	1.96?	<i>J</i> & <i>K'</i>	82	1.5
7C 1754+6420	IRTF	1.09	<i>J</i>	13.5	1.07
7C 1756+6520	IRTF	1.48?	<i>K'</i>	18	0.78
7C 1758+6719	IRTF	2.70	<i>K'</i>	82	0.42
7C 1802+6456	IRTF	2.11	<i>K'</i>	18	0.74
7C 1804+6313	IRTF	?	<i>K'</i>	18	0.80
7C 1805+6332	IRTF	1.84	<i>K'</i>	36	0.63
7C 1807+6841	IRTF	0.82	<i>J</i>	13.5	0.72
7C 1807+6719	IRTF	2.78	<i>K'</i>	36	0.75
7C 1812+6814	IRTF	1.08	<i>J</i>	13.5	0.93
7C 1814+6702	IRTF	4.05?	<i>K'</i>	54	0.78
	Shane		<i>K'</i>	54	1.3
7C 1814+6529	IRTF	0.96	<i>J</i>	13.5	0.84
7C 1820+6657	IRTF	2.98	<i>K'</i>	36	0.69
7C 1816+6605	IRTF	0.92	<i>J</i>	13.5	1.02
7C 1825+6602	IRTF	2.38	<i>K'</i>	18	0.81

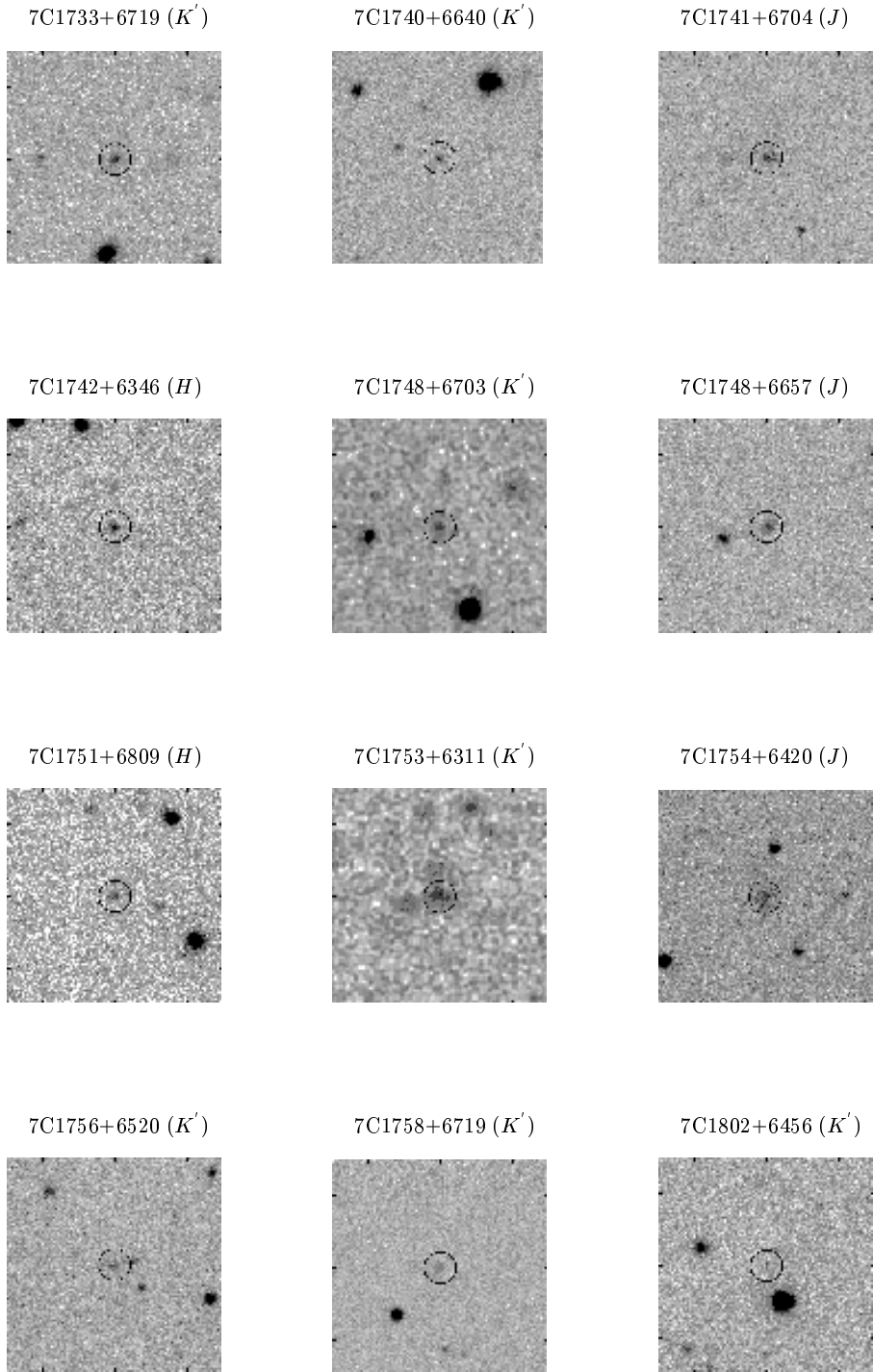


Fig. 1.— Near-infrared images of the  $z > 0.8$  7C sources. The position of each identification is indicated by the dotted circle. The images are  $\approx 30$  arcsec on a side.

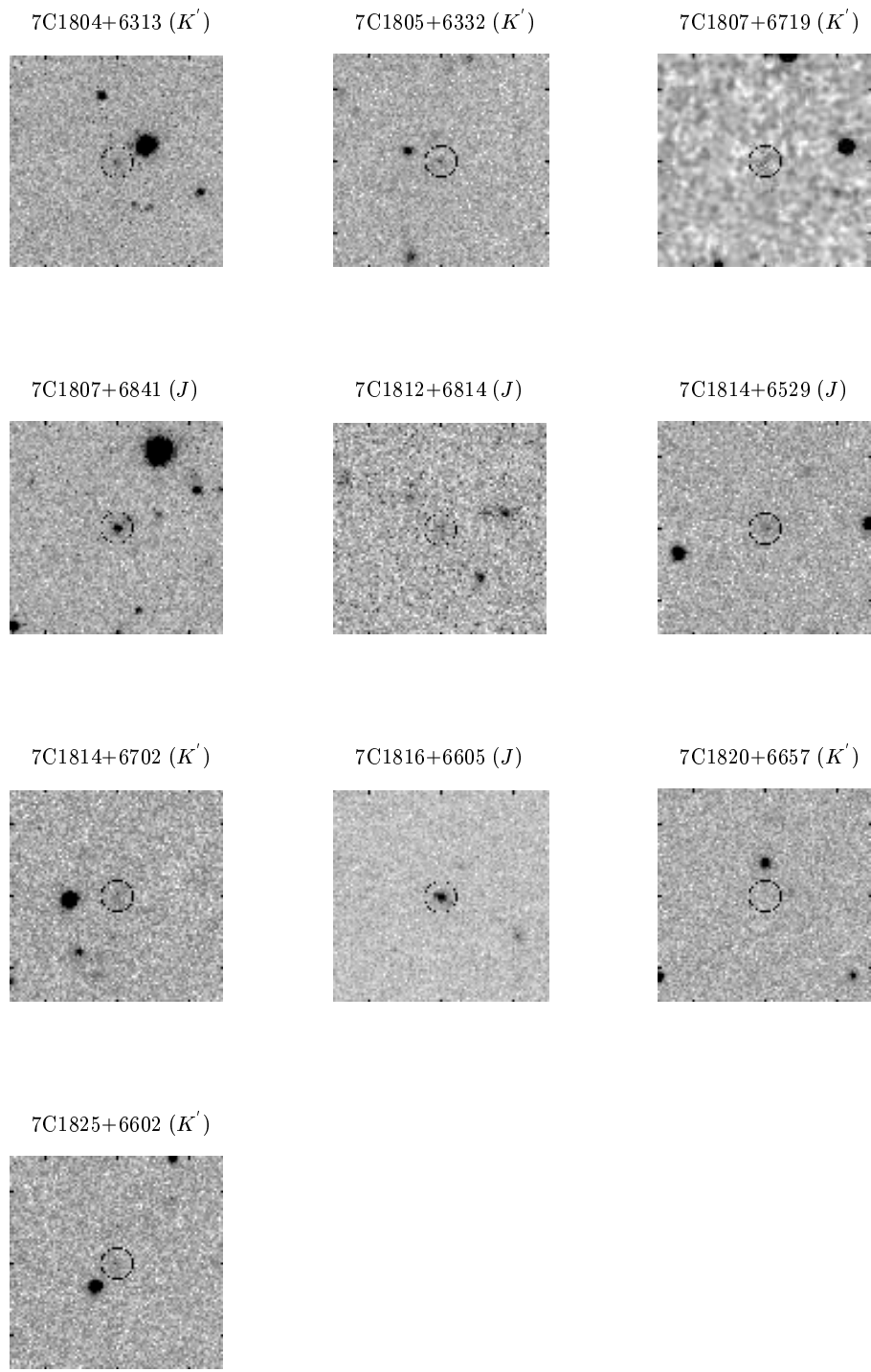


Fig. 1.— continued

### 3. Analysis

#### 3.1. Magnitudes and $k$ -corrections

Aperture magnitudes were measured as listed in Table 2 and corrected to a standard 63.9 kpc metric aperture according to the prescription of Eales et al. (1997), which assumes a power-law curve of growth of the form  $I(< r) \propto r^{0.35}$  for  $z > 0.6$  objects. Our metric aperture corresponds to about 8 arcsec at  $z \gtrsim 1$  in our assumed cosmology, and this angular size is not strongly dependent on the choice of  $\Omega_M$  and  $\Omega_\Lambda$ . For many of our objects we have been able to measure the magnitude in a large aperture, but for some we have had to restrict the aperture to  $\approx 3$  arcsec to avoid contamination from neighbouring objects or excessive noise in the case of faint objects. The aperture correction applied in these cases is  $\approx 0.4$  magnitudes. The disadvantage of this technique is that the aperture magnitude and in particular the correction are scale-size dependent. An alternative would have been to use total magnitudes (cf. Roche et al. 1998). However, we decided against this as for low signal-to-noise detections the curve of growth is ill-defined and can lead to large errors in the magnitudes (Stevens 1999). The mean half-light radius of our objects is 0.9 arcsec, so the typical amount of flux missed in an 8 arcsec aperture will be very small in any case. We thus believe that the use of these large aperture magnitudes will not seriously affect the results of this paper.

For objects with spectroscopic redshifts,  $k$ -corrections to rest-frame  $R$ -band were made using 1Gyr-burst models generated using the PEGASE code (Fioc & Rocca-Volmerange 1997), integrating over the appropriate filter profiles. A model galaxy with a total age of 2 Gyr was used for objects with  $2 < z \leq 3$ , and 3 Gyr for objects with  $0.8 < z \leq 2$ . The  $z > 3$  objects used a 1.4 Gyr-old model galaxy. For most objects the  $k$ -corrections are small ( $< 0.2$  magnitudes), the exceptions to this being the  $z > 3$  objects for which  $K'$  corresponds to rest-frame wavelengths significantly shorter than  $R$ -band (but still above 4000Å) and 7C 1756+6520 which was observed in  $K'$  to check its redshift photometrically. The biggest correction was  $-0.61$  mag. for 7C 1814+6704 at a probable redshift of 4.05.

TABLE 2  
PHOTOMETRY AND SCALE SIZES OF THE 7C-III RADIO GALAXIES

Object	$\phi/''$	Mag.	$M_R$	$r_{\text{hl}}/''$	Range/''	$r_{\text{hl}}/\text{kpc}$	% lines
7C 1733+6719	5	$K' = 18.3 \pm 0.2$	-24.7	1.1	0.46-1.9	9.2	0
7C 1740+6640	3	$K' = 18.9 \pm 0.2$	-24.6	<0.37	-	3.0	17
7C 1741+6704	8	$J = 19.7 \pm 0.2$	-23.6	2.0	0.60-6.2	17	9
7C 1742+6346	3	$H = 19.2 \pm 0.2$	-23.9	<0.5	-	<8.6	7
7C 1745+6624	2	$K' = 20.8 \pm 0.3$	-23.8	-	-	-	10
7C 1748+6703	8	$J = 21.6 \pm 0.3$	-	-	-	-	?
		$K' = 18.3 \pm 0.2$	-	-	-	-	?
7C 1748+6657	8	$J = 19.6 \pm 0.2$	-23.8	0.90	0.58-1.4	7.7	8
7C 1751+6809	3	$H = 19.5 \pm 0.2$	-23.9	0.22	<1.5	1.9	6
7C 1753+6311	3	$J = 20.7 \pm 0.3$	-	-	-	-	?
		$K' = 18.6 \pm 0.2$	-	-	-	-	?
7C 1754+6420	8	$J = 19.1 \pm 0.2$	-24.1	4.5	1.6-13	39	10
7C 1756+6520	3	$K' = 19.2 \pm 0.2$	-	-	-	-	0
7C 1758+6719	8	$K' = 19.3 \pm 0.2$	-24.5	0.35	0.12-1.0	2.6	0
7C 1802+6456	8	$K' = 19.3 \pm 0.3$	-24.1	0.97	0.15-7.0	7.9	50
7C 1804+6313	3	$K' = 19.1 \pm 0.2$	-	-	-	-	?
7C 1805+6332	5	$K' = 19.0 \pm 0.2$	-23.5	1.9	0.52-7.1	16	0
7C 1807+6719	5	$K' = 20.2 \pm 0.3$	-23.9	-	-	-	0
7C 1807+6841	8	$J = 18.8 \pm 0.2$	-23.7	0.87	0.54-1.4	7.2	6
7C 1812+6814	5	$J = 20.4 \pm 0.3$	-22.9	1.1	0.17-10	9.4	5
7C 1814+6702	5	$K' = 19.4 \pm 0.2$	-25.7	-	-	-	0
7C 1814+6529	8	$J = 19.2 \pm 0.15$	-23.9	0.89	0.35-2.3	7.6	<3
7C 1816+6605	5	$J = 18.6 \pm 0.15$	-24.4	0.79	0.56-1.1	6.7	1
7C 1816+6710	5	$H = 19.0 \pm 0.3$					0
7C 1820+6657	3	$K' > 20.7$	>-23.7	-	-	-	>5
7C 1825+6602	5	$K' = 19.0 \pm 0.2$	-24.7	0.59	0.56-0.63	4.6	10

NOTE.—Errors on the magnitudes are estimated assuming a photometric error of 0.1 magnitude combined with noise.  $\phi$  is the aperture diameter and  $M_R$  is measured in a 63.9 kpc metric aperture. The limit on the magnitude of 7C 1820+6657 is a 3- $\sigma$  limit.

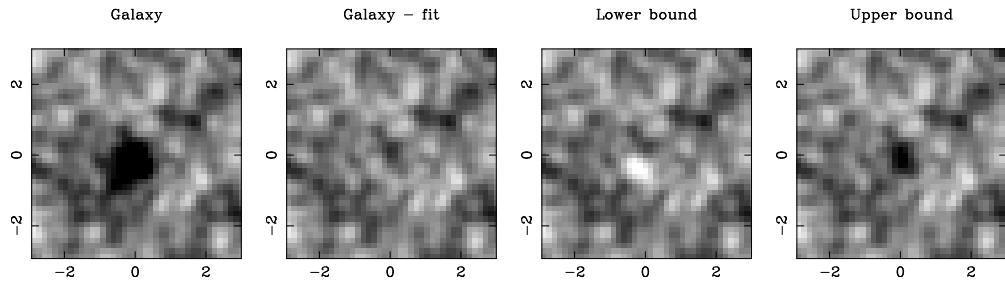


Fig. 2.— An example of the model fitting procedure to the galaxy 7C 1758+6719. The galaxy itself, the residual of the galaxy minus the best fit model ( $r_{\text{hl}} = 0.35$  arcsec) and the galaxy minus the approximate  $\pm 1\sigma$  bounds on  $r_{\text{hl}}$  (0.12 and 1.0 arcsec) are shown, running from left to right. All images have the same symmetric greyscale stretch, with black corresponding to a surface brightness of  $K' = 20.8\text{mag arcsec}^{-2}$ , and the subtractions have been arranged such that each residual image contains zero net flux. Thus a model with too small a scale size results in a compact negative residual near the centre of the image where oversubtraction has occurred, and a model with too large a scale size leaves a compact positive residual near the centre. The flux in the compact residuals left after subtraction of the  $\pm 1\sigma$  models, measured in a 2-arcsec diameter aperture, are  $\pm 0.2$  times the total galaxy flux in the same aperture.

### 3.2. Photometric redshifts for objects in the 7C-III sample

Several of the objects observed had uncertain redshifts [grade  $\gamma$  in Lacy et al. (1999b)] or no redshift information at all. Of the objects without spectroscopic redshifts, 7C 1748+6703 has a  $K'$  magnitude and colours consistent with  $2.4 < z < 4$  whereas 7C 1753+6311 and 7C 1804+6313 both have magnitudes and colours consistent with them having redshifts in the range  $1.2 < z < 1.8$  (Willott et al. 2000). In addition Lacy et al. (1999b) estimated a photometric redshift of 1.7 for 7C 1743+6341. The identification of 7C 1753+6311 in Lacy et al. (1999b), which had a provisional redshift of 1.96, actually corresponds to a blue galaxy along the radio axis. Our Lick image showed that the true identification is a very red ( $R - K' \gtrsim 5$ ) galaxy 4.7 arcsec away which is significantly closer to the likely radio central component. Nevertheless, the original identification may well be associated with the radio galaxy, and the magnitude and colours are consistent with  $z \lesssim 2$ , so we have not revised our redshift estimate. As we aligned the slit with the radio axis, though, we might have expected to see Ly $\alpha$  in the spectrum if the redshift were indeed 1.96. Thus we note that the redshift may well be lower. 7C 1756+6520 had a provisional redshift of 1.48, and its  $K'$  magnitude is just consistent with this, although somewhat fainter than the mean  $K - z$  relation at this redshift. 7C 1814+6702 with a provisional redshift of 4.05 has a  $K'$  magnitude in both the IRTF and Lick data consistent with both  $z \sim 4$  and  $1.2 < z < 1.8$ , although its diffuse and possibly aligned structure is typical of  $z > 3$  objects (van Breugel et al. 1998) so has been kept at 4.05 pending a deeper spectrum. 7C 1816+6710 was observed in  $H$ -band by Lacy et al. (1999a), its magnitude is consistent with its provisional redshift of 0.92. Only one object, 7C 1820+6657, was undetected in our study; its faint magnitude is consistent with its provisional redshift of 2.98.

In summary, we now have photometry on all nine of the high redshift radio galaxies with either no redshift information or uncertain redshifts in the 7C-III sample of 54 objects. All six objects with uncertain redshifts have near-infrared magnitudes consistent with their tentative spectroscopic redshifts. Of the three objects with no redshift

information, two have photometry consistent with them having redshifts  $\sim 1.5$ , and the one remaining object (7C 1748+6703) is probably at  $z \sim 3$ .

### 3.3. Emission line contamination of broadband magnitudes

Line contamination of continuum magnitudes is expected to be small in nearly all the 7C objects, as the correlation of emission line and radio luminosities means that, on average, emission line fluxes will be much less than those from objects in radio-brighter samples. Whereas the  $z \gtrsim 2$  objects studied by Eales & Rawlings (1996) typically have line contaminations of a few tens of percent, the 7C objects, which are selected at radio fluxes about four to five times lower, should have line contaminations  $\lesssim 10\%$ . We have listed in Table 2 the estimated percentage contribution to the observed flux for all objects with bright emission lines in the observed band. These are based on the spectroscopy of Lacy et al. (1999b), using the median Ly $\alpha$ /H $\alpha$ +[NII] ratio of 0.7 in Eales & Rawlings (1996), the line ratios in the composite radio galaxy spectrum of McCarthy (1993) and the H $\alpha$ /H $\beta$  ratios of Koski (1978) to estimate the strengths of lines falling in the observed near-infrared. As expected, most objects have emission line contributions of  $< 10\%$ . For only one object, 7C 1802+6456, is the emission line contamination expected to be  $> 20\%$ .

### 3.4. Estimation of half-light radii

The seeing during most of our IRTF observations was very good, and it was clear from looking at the images that there was a wide range in the scale sizes of the hosts. We therefore selected a subsample consisting of the 15 sources with grade  $\alpha$  or  $\beta$  redshifts in the range  $0.8 < z < 2.7$  in Lacy et al. (1999b) for which we had IRTF images. Although not complete, this sample should be representative of the 7C objects in this redshift range. To estimate the scale sizes we convolved model elliptical (de Vaucouleurs) galaxies having a range in half-light radius  $r_{\text{hl}}$  from 0.1 to 6.7 arcsec and zero ellipticity with a PSF from a nearby star in each IRTF image. The model was subtracted from the data and the minimum in the sum of the squares of the residuals found, along with the approximate  $\pm 1\sigma$  range. An example of this process is shown in Fig. 2. The results were

also checked by eye to see that the fits were reasonable. Nearby companion objects and discrete sub-components were subtracted prior to the fits. Although this is far from a full host galaxy model (in particular we made no attempt to discriminate between disc and de Vaucouleurs fits), we feel that it should give a fair estimate of the scale size, and was all that the signal:noise in the images typically justified.

To obtain a major axis scale size to compare to other work, we need to assume a mean ellipticity,  $e$ , and correct our scale sizes with this. Roche et al. and Govoni et al. (2000) derive very similar mean values of  $e \approx 0.2$  for the 6C radio galaxies at  $z \sim 1$  and nearby radio galaxy hosts respectively, so this value has been assumed to correct the mean scale sizes quoted in Section 4 by multiplying the scale size by the square root of the axial ratio corresponding to  $e = 0.2$ , namely 1.06.

For two objects we have been able to compare the scale sizes with those measured on images taken with the Hubble Space Telescope (HST). 7C 1758+6719 ( $z = 2.70$ ) was observed with WFPC2 through the F702W filter; details of the observations will be given in a future paper (Lacy et al. in preparation). For this rest-frame UV image an exponential disk with  $r_{\text{hl}} = 0.21$  arcsec was found to be a good fit to the radial profile. This can be compared with the estimate of  $r_{\text{hl}}$  from the IRTF image of 0.35 arcsec with a  $1\sigma$  range of 0.12 – 1.0 arcsec, which we consider fair agreement. 7C 1754+6420 ( $z = 1.09$ ) was observed through the F675W filter (Ridgway & Lacy in preparation). Again, the rest-frame UV emission was better fit by a disk than a de Vaucouleurs profile. In this case the scale size came out significantly smaller than the estimate from the IRTF image, 0.7 arcsec in the HST image compared to a best fit of 4.5 arcsec and a range of 1.6 – 13 arcsec for the IRTF image. This was despite the subtraction of a nearby companion to the south which was successfully removed from both the HST and IRTF images. The cause of this discrepancy is not clear. This image had the worst seeing of any of our IRTF images (1.1 arcsec), but the scale size measured in the IRTF image is much larger than the seeing HWHM. The radial profile of the IRTF image is, however, not at all well fit by the disk model from the HST image. Therefore perhaps the most likely cause of this discrepancy is that

the galaxy has a UV-bright disk component embedded in a much larger scale-size elliptical.

### 3.5. Other data from the literature

To increase the number of high redshift objects in our study we have added the results of photometry of  $z \sim 2 - 5$  radio galaxies by van Breugel et al. (1998). We also estimated scale sizes from their figure 2 for objects which appeared to be dynamically-relaxed ellipticals (seven out of the eight of their radio galaxies with  $z < 3$ ). We applied  $k$ - and aperture corrections in a consistent manner to that for the 7C-III radio sources. We have also added those  $1.6 < z < 2.4$  objects without a strong point source contribution from the NICMOS study of radio galaxies by Pentericci (1999; and Pentericci et al. 2000), including the estimates of scale sizes for the five out of the nine objects in this redshift range for which Pentericci considers it possible to fit meaningful scale sizes. We also include the low luminosity  $z = 4.42$  radio galaxy VLA 123642+621331 discovered in the flanks of the Hubble Deep Field (Waddington et al. 1999) and 53W002 at  $z = 2.239$  (Windhorst, Mathis & Keel 1992).

The resulting high redshift (HZ) sample is detailed in Table 3. It mostly contains objects of radio luminosity comparable to the 3C radio galaxies at  $z \sim 1$ . As these objects (particularly those at  $z > 3$ ) were generally observed outside of rest-frame  $R$ -band, and are mostly not from complete samples, the results including the HZ sample will not be as reliable, though as we shall see the same trends seem to exist with or without this sample.

## 4. Discussion

### 4.1. Radio-luminosity and redshift dependence of absolute magnitudes

In Fig. 3 we plot the rest-frame  $R$ -band magnitudes against redshift for several samples of radio galaxies. We plot the  $z > 0.8$  7C-III objects with spectroscopic redshifts and infrared imaging,  $z > 0.8$  6C radio galaxies with photometry from Eales et al. (1997),  $z > 0.8$  3C radio galaxies in the Laing, Riley & Longair (1983; LRL) complete sample with photometry from Best, Longair & Röttgering (1998) [apart from 3C22 which is a lightly-reddened quasar (Rawlings et al. 1995) and therefore excluded from the sample, 3C 175.1

TABLE 3

THE “HZ” SAMPLE OF OTHER HIGH REDSHIFT RADIO GALAXIES FROM THE LITERATURE

Object	$z$	$\phi/''$	Mag.	$M_R$	$r_{\text{hl}}/''$	% lines	ref.
6C 0140+326	4.41	8	$K_s = 20.0$	-25.5		10	1
MRC 0152-209	1.89	4	$H = 18.7$	-25.3	0.2	6	2
MRC 0156-252	2.09	4	$H = 18.4$	-25.9		5	2
USS 0211-122	2.34	4	$H = 19.6$	-25.0	0.73	3	2
MRC 0324-228	1.89	4	$H = 19.9$	-24.1		0	2
4C 60.07	3.79	8	$K' = 19.3$	-25.4		0	1
4C 41.17	3.80	8	$K_s = 19.2$	-25.5		0	1
B3 0744+464	2.926	8	$K_s = 18.5$	-25.5	0.92	0	1
MRC 0943-242	2.922	8	$K = 19.2$	-24.8	0.70	0	1
MG 1019+0534	2.765	8	$K = 19.1$	-24.7	0.97	0	1
3C 257	2.474	8	$K = 17.8$	-25.7	1.55	35	1
VLA 123642+621331	4.424	1.5	$K = 21.4$	-24.8	0.29	0	3
4C 1243+036	3.581	8	$K = 19.3$	-25.2		0	1
USS 1410-001	2.33	4	$H = 19.3$	-25.4		9	2
8C 1435+635	4.251	8	$K = 19.5$	-25.7		0	1
MRC 1707+105	2.35	4	$H = 18.3$	-24.5	1.62	0	2
53W002	2.239	-	$K = 19.2^a$	-24.1	1.1	20	4
MRC 2025-218	2.630	8	$K' = 18.5$	-25.2	0.64	0	1
MRC 2048-272	2.06	4	$H = 20.2$	-24.1	0.64	0	2
MG 2121+1839	1.861	8	$K = 18.7$	-24.1	3.07	0	1
MG 2144+1929	3.594	8	$K' = 19.2$	-25.3		0	1
TX 2202+128	2.704	8	$K = 18.4$	-25.4	0.19	0	1
MRC 2224-273	1.68	4	$H = 19.2$	-24.4	0.2	28	2
4C28.58	2.905	8	$K = 18.7$	-25.3		0	1

<sup>a</sup>Total magnitude

NOTE.—References: (1) van Breugel et al. (1998); (2) Pentericci (1999); (3) Waddington et al. (1999); (4) Windhorst et al. (1992)

( $z = 0.92$ ) which has photometry from Ridgway & Stockton (1997) and 3C 263.1 ( $z = 0.824$ ) which has photometry from Eales (personal communication)]. We have also added local radio galaxies in LRL from Owen & Laing (1989) and the HZ sample of galaxies of Table 3. All these objects, with the exception of three FRIs out of the 24 objects in the Owen & Laing LRL sample are either FRII or compact steep-spectrum sources. All the  $z > 0.8$  7C-III sources at  $z > 0.8$  are well above the FRI/FRII boundary in radio luminosity, with  $L_{R(151)} \gtrsim 10^{26} \text{WHz}^{-1} \text{sr}^{-1}$  compared to the FRI/FRII boundary at  $L_{R(151)} \sim 10^{25} \text{WHz}^{-1} \text{sr}^{-1}$ .

There is a clear trend for redshift and absolute magnitude to correlate, even if the incomplete HZ sample is excluded. The 3C, 6C and 7C samples are all complete samples, selected on the basis of low frequency radio flux only, and are nearly completely identified. Thus the only selection effect which needs to be considered for these samples is the tendency for redshift and luminosity to correlate within each flux limited sample. With the wide range in radio luminosities in the complete samples at  $z \sim 1$ , however, we can separate out the luminosity dependence. This is illustrated in Fig. 4, where we have plotted absolute magnitude against radio luminosity for 3C, 6C and 7C galaxies in the redshift range  $0.8 < z < 1.4$ . In this redshift range the mean magnitude in 3C is  $M_R = -24.17 \pm 0.13$ , whereas in 6C it is  $-23.79 \pm 0.14$  and in 7C-III  $-23.78 \pm 0.15$ . This suggests that only the most radio-luminous objects have slightly brighter (by  $\approx 0.4$  mag) hosts [see also Rawlings et al. (1998) where preliminary  $K$ -band photometry on the 7C-I and 7C-II samples is presented].

We can think of two possible explanations for this radio luminosity dependence of host magnitude at  $z \sim 1$ . The first is a contribution from AGN-related light, e.g. emission lines and reddened and/or scattered quasar light (Eales & Rawlings 1996). Rigler et al. (1992), however, show that the fraction of emission from  $z \sim 1$  3C radio galaxies which is aligned with the radio jet axis, and therefore probably closely related to the AGN activity, contributes only  $\approx 10\%$  of the light in the observed  $K$ -band. Also, Simpson, Rawlings & Lacy (1999) argue that reddened quasar light is responsible for  $\lesssim 10\%$  of the observed near-

infrared emission from 3C radio galaxies on the basis of  $3\mu\text{m}$  imaging. Thus we believe that only  $\sim 10 - 20$  per cent of the host luminosity can be accounted for by the AGN, not the  $\approx 40$  per cent required to explain the higher host luminosities of the 3C galaxies. The second possibility is that the radio luminosity may be correlated with the mass of the host. This could arise, for example, if correlation of black hole mass and the mass of the spheroidal component of galaxies which is claimed to be present at low redshift (e.g. Magorrian et al. 1998) is appearing at the highest radio luminosities (Roche et al. 1998). We have argued (Lacy, Ridgway & Trentham 2000; see also Willott et al. 1999) that most radio galaxies are sub-Eddington accretors, but at the highest luminosities corresponding to the highest black hole masses, even the radio galaxies may be accreting at near Eddington rates. Thus at these highest luminosities we might expect a host galaxy mass - AGN luminosity (and therefore host luminosity) correlation to appear. Also, the mass of the host may correlate with the density of the intergalactic medium confining the radio source, which would enhance the radio luminosity.

We have made a crude model of the luminosity dependence by assuming a contribution from AGN-related light to a base host optical luminosity  $L_0$ . We model this contribution as a combination of a component due to emission lines and another component due to other AGN-related light. (We separate the emission line contribution, as the equivalent width of the emission lines is a strong function of redshift, unlike the other AGN-related emission which we expect to be much less redshift dependent.) Both these components should be proportional to the AGN luminosity, which we assume to be proportional to  $L_{R(151)}$  to the power 0.8 (Serjeant et al. 1998; Willott et al. 1999), i.e.

$$L_{\text{host}}(z) = L_0(z) + (\alpha + \beta(z))L_{R(151)}^{0.8}, \quad (1)$$

where  $\alpha L_{R(151)}^{0.8}$  is the contribution of AGN-related light other than emission lines and  $\beta(z)L_{R(151)}^{0.8}$  is the contribution due to emission lines. The base host luminosity at  $z \approx 1$  was set to  $L_0(1) = 10^{23} \text{WHz}^{-1}$ , or  $M_R \approx -23.7$ , close to the mean of the 7C and 6C data, and  $(\alpha + \beta(1))$  fit by eye to be  $\approx 3.5 \text{W}^{0.2} \text{Hz}^{-0.2}$  (Fig. 4). The emission line contribution to the total near-infrared luminosities of the 3C radio galaxies at these redshifts is  $\sim 10\%$

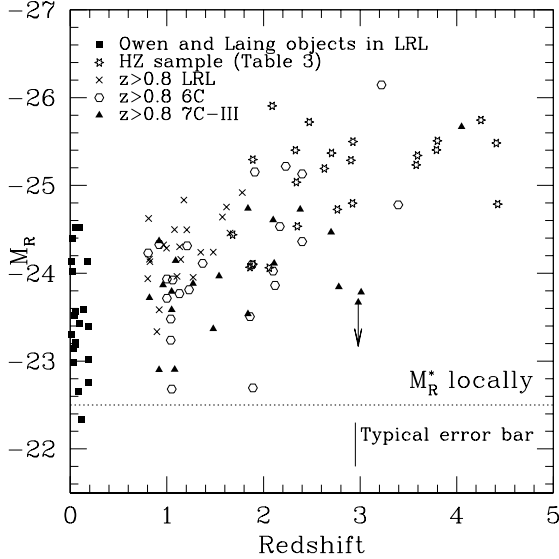


Fig. 3.— The rest-frame  $R$ -band absolute magnitudes. The value of  $M_R^*$  locally is indicated by the dotted line. A typical error bar for the 7C objects is indicated; the other samples generally have smaller error bars.

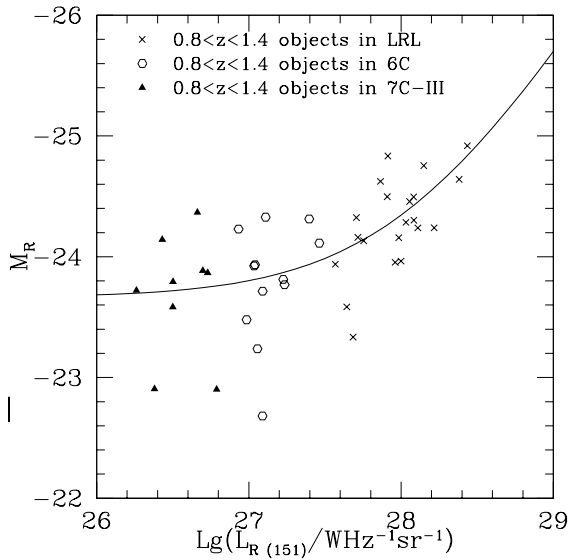


Fig. 4.— The luminosity dependence of host galaxy magnitude at  $z \sim 1$ . The line represents the model of equation (1).

(Rawlings et al. 1997; Rawlings Eales & Lacy 1990), or about 20% of the overall luminosity-dependent correction. We have therefore set  $\alpha = 2.8 \text{ W}^{0.2} \text{ Hz}^{-0.2}$  and  $\beta(1) = 0.7 \text{ W}^{0.2} \text{ Hz}^{-0.2}$ .

Using this formula we can then correct the host magnitudes for AGN-related light and produce plot of  $L_0$  versus redshift. [Rather than attempt to model the redshift dependence of  $\beta$  we have used emission line contamination estimates from Eales & Rawlings (1997) and van Breugel et al. (1998) to explicitly correct the magnitudes in the 6C and high redshift samples (where these were unknown the object was omitted from the plot and correlation analysis), and our own estimates to correct the 7C-III magnitudes.] The results are shown in Fig. 5, which shows that there is indeed a correlation of  $L_0$  with redshift. This was confirmed using the Kendall Tau statistic generalized to include limits, as implemented in the IRAF.STSDAS program BHKMETHOD (Isobe & Feigelson 1990), which returned a  $\tau = 0.52$  for the 106 objects from the 3C, 6C, 7C and HZ samples after correction. This corresponds to a probability that there is *no* correlation between  $L_0$  and redshift of  $< 0.0001$ . However, this probability increases to 0.13 if the HZ sample is removed. We have also conducted the same statistical test before correction for radio luminosity-dependent effects in equation (1). This gave a  $\tau = 0.95$  and a probability of no correlation of  $< 0.0001$ , removing the HZ sample reduced this to  $\tau = 0.66$ , again with the probability of no correlation of  $< 0.0001$ .

#### 4.2. The dispersion in the host luminosities

The low scatter in the magnitudes of radio galaxies in the  $K - z$  Hubble Diagram out to  $z \gtrsim 3$  has long been used as an argument for a high redshift of radio galaxy formation (e.g. Lilly 1989). This low scatter is thought to come about because radio galaxies form at  $z > 3$  then evolve along similar passive evolution tracks to end at radio galaxy hosts today. With a few modifications this simple picture still seems to be basically valid. Fig. 3 and Table 4 show that the dispersion in absolute magnitudes to  $z \sim 4$  is indeed very low. After correction for AGN-contamination, however, the dispersion in  $L_0$  for the  $z > 1.8$  objects seems to be higher than for the uncorrected objects (Table 4). As discussed above, the correlation of absolute

magnitude with redshift is also less tight after correction.

At first sight it seems paradoxical that correction for luminosity-dependent effects should *increase* the scatter in the absolute magnitudes. However, this can be understood if the luminosity-dependent contributions  $(\alpha + \beta)L_R^{0.8}$  are approximately equal to the highest values of  $L_0$ . (The  $z > 1.8$  objects have a very narrow range in  $L_R$  as the range in flux of these objects is low, all except VLA 123642+621331 having 151 MHz fluxes between 0.5 and 10 Jy.) The addition of the luminosity-dependent contributions can then boost the objects with low  $L_0$  by a significant factor, whereas the addition to the objects with high  $L_0$  results in only a relatively small fractional increase in the luminosity (see also de Vries 1999). The result of this is a reduction of the scatter in the total luminosities.

We have used the F-test for variances to examine the statistical significance of the increase in scatter of the  $L_0$  values. Comparing the objects with  $0.8 < z < 1.8$  to those with  $1.8 < z < 2.8$ , we find that the increase in the sample standard deviation from  $\sigma_{n-1} = 0.53$  to  $\sigma_{n-1} = 0.93$  is significant at the 0.1 % level. At  $z > 2.8$ , our sample contains two upper limits on the magnitudes, so we give a lower limit to the scatter of  $\sigma_{n-1} > 0.97$ . This is again significantly higher than that in the range  $0.8 < z < 1.8$  (at the 0.2 % level). Thus there is good evidence that the scatter in  $L_0$  is increasing with redshift, suggesting that we are close to the formation epoch of at least a significant fraction of the radio galaxy population.

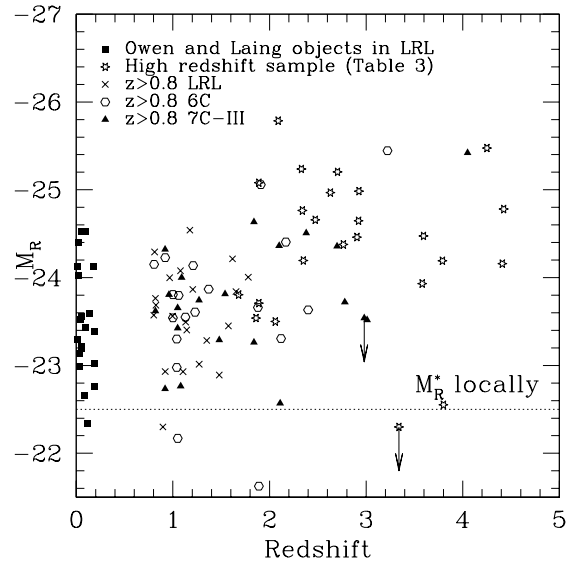


Fig. 5.— The redshift dependence of radio galaxy absolute magnitude after approximate correction for enhancements which correlate with radio luminosity, including emission lines.

Table 4: Scatter in radio galaxy absolute magnitudes as a function of redshift

Redshift range	$n^a$	Mean $M_R$		$\sigma_{n-1}^b$	
		uncorrected	corrected	uncorrected	corrected
$0.8 \leq z < 1.8$	44	-24.0	-23.6	0.5	0.5
$1.8 \leq z < 2.8$	25	-24.6	-24.2	0.7	0.9
$z \geq 2.8$	15	>-24.3	>-25.1	>0.7	>1.0

<sup>a</sup>Number of objects in each sub-sample

<sup>b</sup>Standard deviation of the sample.

NOTE.—  $M_R$  is measured in a 63.9 kpc metric aperture. Uncorrected magnitudes have  $k$ -corrections only, no corrections for emission line or AGN luminosity have been applied. Corrected magnitudes have, in addition to  $k$ -corrections, emission-line contamination corrections and a correction for AGN luminosity as detailed in Section 4.1.

### 4.3. The scale sizes of the hosts

Roche et al. (1998) have shown that the scale sizes of the  $1 < z < 1.4$  6C galaxies are significantly smaller than their more radio luminous 3C counterparts as measured by Best et al. (1997), suggesting a strong dependence of scale size on AGN luminosity. In this section we re-examine this using our data on the 7C objects, and further data on 3C scale sizes published recently.

To compare with the 6C results, we have defined complete samples of 7C-III and 3C radio galaxies from LRL in the redshift range  $0.8 < z < 1.4$  (we took the lower limit of 0.8 so as to include more 3C and 7C objects; only two 6C objects lie in the redshift range  $0.8 < z < 1$ , and we do not feel their exclusion will significantly affect the results). For the 3C objects we have used size estimates from the 2D modelling of McLure & Dunlop (2000) or the Keck  $K$ -band images of Ridgway & Stockton (1997) where available, and otherwise from Best et al. (1997). No estimates were available for three of the sixteen objects in the 3C sample, and we have omitted 3C356 due to confusion over the true identification. One of the objects missing from the 3C sample were omitted from the sample of Best et al. (1997) (3C 263.1), and the other two, 3C 13 and 3C 368 have  $K$ -band structures which are clearly affected by AGN-related emission as they are closely aligned with the radio axes. Of the 7C-III objects, only one, 7C 1816+6710, has no scale size estimate as its image was taken in poor seeing, although the scale size of 7C 1742+6346 is an upper limit only. All the 7C scale sizes were increased by a factor of 1.06 to correct for an expected mean ellipticity of 0.2.

In Fig. 6 we plot the scale sizes of the 3C, 6C and 7C radio galaxies in the samples defined above against host absolute magnitude. Although the scatter is large it does seem that the 7C-III radio galaxies have scale sizes consistent with their magnitudes when compared to the 3C radio galaxies, although the 6C objects are plotting below the general trend. The mean scale size for the 3C sample is  $11.1 \pm 1.4$  kpc and that for the 6C sample  $4.7 \pm 0.9$  kpc. For the 7C-III sample, we find a median scale size of  $0.9 \pm 0.4$  arcsec, which, when corrected for a mean ellipticity of 0.2, corresponds to about  $8 \pm 3$  kpc. (Using the whole subset of 7C-III sources in the range  $0.8 < z < 2.7$  with

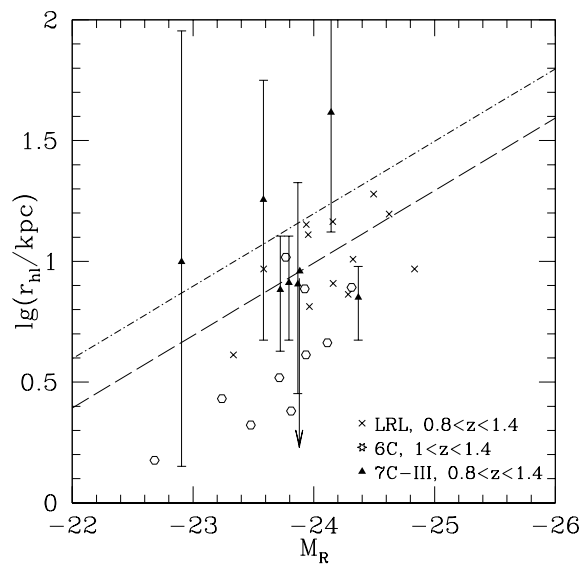


Fig. 6.— The dependence of half-light radius on host absolute magnitude. Errors are shown for the 7C objects only. The dot-dashed line represents the correlation observed for local ellipticals (equation (2) with  $\Delta R = 0$ ); the dashed line the same relationship corrected to  $z \sim 1$  using the mean properties of the 3C hosts (i.e. with  $\Delta R = 0.68$ ).

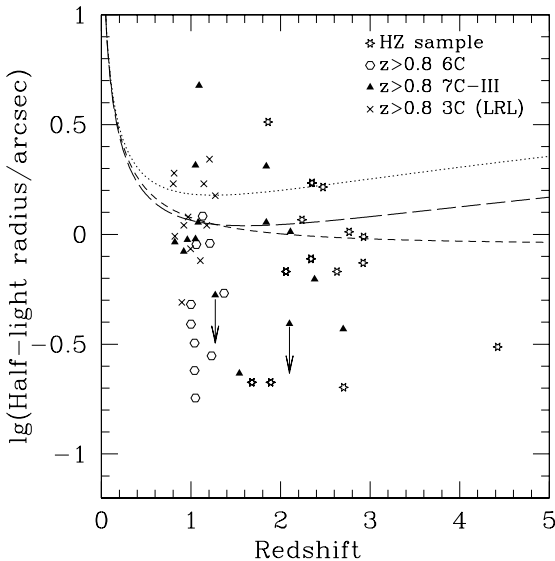


Fig. 7.— Half-light radius in arcseconds versus redshift. The lines show the angular size of a standard rod of length equal to the mean of the half-light radii of local FRII host galaxies (13 kpc) as a function of redshift in an  $\Omega_M = 1, \Omega_\Lambda = 0$  cosmology (dotted line), an  $\Omega_M = 0.3, \Omega_\Lambda = 0.7$  cosmology (long-dashed line) and an  $\Omega_M = 0, \Omega_\Lambda = 0$  cosmology (short-dashed line).

measured scale sizes we obtained the same result.) The mean for the 7C-III is thus between that of the 6C and 3C samples, and statistically consistent with both.

A further check is provided by the effective-radius – galaxy magnitude relationship discussed by Roche et al. (1998),

$$\lg(r_{hl}/\text{kpc}) = -0.3(M_R + \Delta R + 20.01), \quad (2)$$

where  $\Delta R$  is the amount by which the hosts have brightened by passive evolution from  $z = 0$ . To set  $\Delta R$ , we used the mean scale size of the 3C galaxies in our  $0.8 < z < 1.4$  sample of 11.1 kpc, and the mean magnitudes of the same objects using the photometry of Best et al. (1998). This gave  $\Delta R = 0.68$ . We have plotted the relationship of equation (2) on Fig. 6, for both  $\Delta R = 0$  and  $\Delta R = 0.68$ . The 7C radio galaxies are consistent with this relation for  $\Delta R = 0.68$  (within the scatter), but most of the 6C radio galaxies plot significantly below the line.

We therefore believe that a combination of poor seeing in both the Roche et al. (1998) and Best et al. (1998) studies, which lead to poor scale size estimates, combined with small number statistics in the Roche et al. study, can probably explain the result of Roche et al. without the requirement for scale-size to depend very strongly on radio luminosity, though clearly better images of both the 6C and 7C objects will be needed to be certain of this.

We have also investigated possible redshift dependences of scale size with the addition of data on objects in the HZ sample listed in Table 3. Fig. 7 shows the results of plotting the scale size in arcsec against redshift. The mean half-light radius for local hosts of classical double FRIIs from Owen & Laing (1989) and Govoni et al. (2000),  $\approx 13 \pm 2.5$  kpc, is also plotted as a line in this figure for three different cosmologies. There is some evidence for a weak trend for scale size to decrease with increasing redshift, but with a lot of scatter. In an attempt to reduce the scatter we have tried using a correction based on equation (1), by introducing a correction in the log of the scale size:

$$\Delta \lg r_{hl} = -0.3(M - M_0(z)),$$

where  $M$  is the absolute  $R$ -band magnitude after correction for line contamination, and  $M_0(z)$  is

$L_0(z)$  converted to absolute magnitude. With this correction, using the 7C, 6C, 3C ( $0.8 < z < 1.4$ ) and HZ samples there is a weak anticorrelation of scale size with redshift, significant at about the 5% level using the BHKMETHOD.

Inspection of Fig. 7, and the comparison to low redshift FRII hosts, shows that the scatter in scale sizes is large at all redshifts, and suggests that any evolution in scale size is weak. FRI hosts at low redshift, however, have significantly brighter hosts and larger scale sizes at a given radio luminosity (e.g. Owen & Ledlow 1994), suggesting that merging in the richer cluster environments associated with these objects may be significant if they are the descendants of more luminous sources at high redshift. An argument against this is provided by a recent study of brightest cluster galaxies (BCGs) by Burke, Collins & Mann (2000), who show that, when selection effects are properly taken into account, the BCGs of the most X-ray luminous clusters brighten with redshift (to a similar extent as the FRII hosts, in fact), and thus there is little evidence of significant merger activity for redshifts  $0 < z < 1$ . However, because the FRII hosts are significantly less luminous than BCGs, mergers that would enhance the luminosity of a BCG by only a few percent would enhance that of an FRII host by a much larger factor. Nevertheless, the lack of evidence for merger activity in even rich clusters suggests that FRII hosts, which are generally found in poor cluster environments (e.g. Wold et al. 2000), are probably not significantly affected by merging, at least at  $z < 1$ .

#### 4.4. Surface brightness evolution

To demonstrate that the redshift dependence of host magnitude is independent of the assumed cosmology we have plotted in Fig. 8 the effective surface brightness (defined here as the flux within  $r_{\text{hl}}$  divided by  $\pi r_{\text{hl}}^2$  converted into magnitudes) in the rest-frame  $R$ -band versus redshift for the sub-sample of 7C-III galaxies with estimated scale sizes. We have compared this to the cosmological surface brightness dimming expected in a standard expanding Universe with a Friedmann-Robertson-Walker metric. The surface brightness decreases with redshift much less rapidly than the prediction for a non-evolving stellar population (solid line in Fig. 8). This demonstrates that the brightening of the hosts with redshift is a real evolutionary ef-

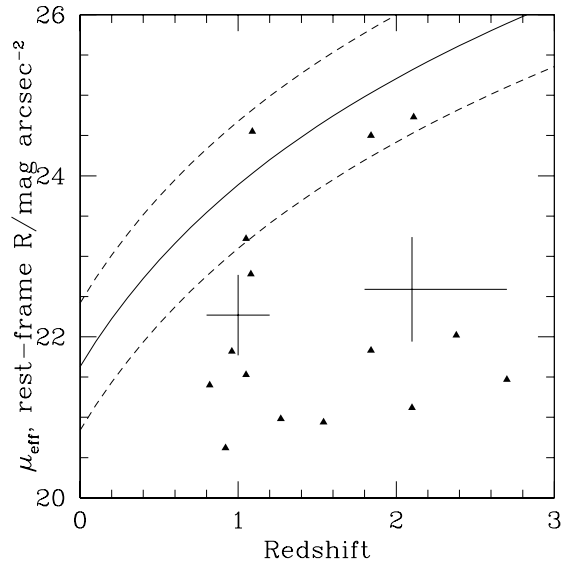


Fig. 8.— The effective surface brightness as a function of redshift for the  $0.8 < z < 2.7$  7C-III galaxies observed with the IRTF, after correction for emission line contamination. The crosses are the mean values of the surface brightness in the redshift range indicated by the horizontal bars and with an error in the mean indicated by the vertical bar. The mean local value for FRII radio galaxies from Govoni et al. (2000) and its expected behaviour with redshift is indicated by the solid line, with the dashed lines showing the  $\pm 1\sigma$  range.

fect, and not one produced by an incorrect choice of  $\Omega_M$  and  $\Omega_\Lambda$ .

## 5. The evolution of radio galaxy hosts

The evolution of host magnitude and rest-frame surface brightness with redshift, the lack of strong evolution in scale sizes in the subset of objects with “undisturbed” morphologies, and the low scatter ( $< 1$  magnitude) in the absolute magnitudes up to at least  $z \sim 3$  are all consistent with an early formation epoch ( $z \gtrsim 3$ ) for most, and perhaps all, radio galaxy hosts. At first sight these results are in conflict with standard CDM-based models for galaxy formation, in which hierarchical structure formation occurs in a “bottom up” fashion with the most massive galaxies forming late. Radio galaxies at  $z \sim 2$  are much brighter than the average quasar host predicted by the models of Kauffmann & Haehnelt (2000), for example. To compare our radio galaxy sample to these predictions we have assumed an equivalent quasar luminosity equal to the mean of the  $1 < z < 3$  7C quasars,  $M_B \approx -25$  (Willott et al. 1998). For quasars of this luminosity, the Kauffmann & Haehnelt models predict a mean host magnitude of  $M_V \approx -21.5$  compared to our radio galaxies with a luminosity-corrected median  $M_R \approx -23.5$  (corresponding to  $M_V \approx -23$ ). In contrast, the hosts of radio-quiet quasars at  $z \sim 2$  seem to fit this model quite well (Ridgway et al. 2000).

Between  $z \sim 1.3$  and  $z \sim 2.3$ , there is evidence for an increasing scatter in base host luminosity. This suggests we are close to the formation epoch at  $z \sim 2.3$ . There are two other pieces of evidence which point to strong evolution in the host galaxies and which appear at  $z \gtrsim 2.5$ . First, the observations of Pentericci (1999; and Pentericci et al. 2000) and van Breugel et al. (1998) show that the morphologies of radio galaxy hosts at  $z < 2.5$  are mostly relaxed ellipticals, whereas at higher redshifts ( $z > 2.5$  in the HST NICMOS  $H$ -band images of Pentericci et al. and  $z > 3$  in the ground-based  $K$ -band images of van Breugel et al.) hosts with clumpy structures aligned with the radio source axis become much more common<sup>2</sup>. Second, the detection rate of continuum

submillimeter emission from hot dust seems to rise rapidly at  $z > 2.5$  (Archibald et al. 2000). The 6C and 7C samples are completely identified with luminous host galaxies out to at least  $z \approx 3$ , however, which would suggest the bulk of the stars had formed and/or merged onto the host by  $z \sim 3$ . One way around a high formation redshift for all objects would be to assume a systematic delay between a host forming the bulk of its stars and the switching on of powerful radio jets (for example, if the black hole needs time to accrete enough mass). Radio galaxies would then always be seen with luminous hosts. However, the strong evolution in the hosts seen by van Breugel et al. around  $z \sim 3$  suggests that their nature is still changing up to at least that epoch.

Taken together, the evidence suggests that the epoch of radio galaxy host formation was essentially over by  $z \sim 3$ , in the sense that most objects had formed the bulk of their stars, although further star-formation and merger activity continued in many objects up to  $z \sim 2$ . As radio galaxies can be found out to  $z > 5$ , however (van Breugel et al. 1999), and there is no sign of a substantial drop in the space density of radio galaxies out to  $z > 4$  relative to their peak space density at  $z \sim 2.5$  (Jarvis et al. 1999), this formation epoch must last at least a Gyr. In contrast, field ellipticals with evolved stellar populations and luminosities  $\sim L_*$  seem to become rarer at  $z > 1$  (Zepf 1998; Barger et al. 1999; Dickinson 1999), suggesting a later formation epoch, perhaps  $z \sim 1 - 2$ .

A recent variation on the hierarchical models, the so-called Anti-Hierarchical Baryonic Collapse Model (Granato et al. 2000) may be able to explain these observations. This predicts that the massive hosts of powerful AGN may have formed at  $z \sim 3$ . This model uses the same CDM assumptions as the standard scenarios, but assumes that the dense gas in the most massive haloes can collapse and form stars in a massive spheroidal component more rapidly than that in the smaller haloes associated with normal galaxies. Star formation is switched off in these objects by winds from the AGN and the starburst at high redshift. If radio galaxy hosts are indeed typical of the most massive elliptical galaxies and their progeni-

<sup>2</sup>van Breugel et al. argue that this is not simply due to the  $z > 3$  objects being observed at shorter rest-frame wavelengths, as lower redshift objects observed at the same rest-

frame wavelengths as the  $z > 3$  objects still look like relaxed ellipticals.

tors this model should be applicable to them, and would explain their anomalous evolution relative to generally less luminous field ellipticals.

We thank Wim de Vries, Michael Gregg and Wil van Breugel helpful discussions, the referee for a useful report, and the staff at the IRTF and Lick Observatory for their assistance. We are also very grateful to Chris Willott for providing the photometric redshift estimates for those 7C-III radio galaxies without spectroscopic redshifts prior to publication. The IRTF is operated by the University of Hawaii on behalf of NASA. AJB acknowledges support from the Cambridge Institute of Astronomy PPARC observational rolling grant, ref. no. PPA/G/O/1997/00793, and a NICMOS postdoctoral fellowship while at Berkeley (grant NAG 5-3043). This work was performed under the auspices of the U.S. Department of Energy by University of California Lawrence Livermore National Laboratory under contract No. W-7405-Eng-48, and was partly based on observations with the NASA/ESA Hubble Space Telescope, obtained at the Space Telescope Science Institute, which is operated by the Association of Universities for Research in Astronomy, Inc. under NASA contract No. NAS5-26555.

## REFERENCES

Archibald E.N., Dunlop J.S., Hughes D.H., Rawlings S., Eales S.A., Ivison R.J., 2000, MNRAS, submitted (astro-ph/0002083)

Barger A.J., Cowie L.L., Trentham N., Fulton E., Hu E.M., Songaila A., Hall D., AJ, 117, 102

Best P.N., Longair M.S., Röttgering H.J.A., 1997, MNRAS, 292, 758

Burke D.J., Collins C.A., Mann R.G., 2000, ApJL, in press (astro-ph/0002185)

de Vries W., 1999, PhD thesis, University of Groningen

Dickinson M., 1999, in, Hammer F., et al., eds, Building Galaxies: From the Primordial Universe to the Present, Proceedings of the XIXth Moriond Astrophysics Meeting. Ed. Frontières, p. 257, in press

Eales S.A., Rawlings S., 1993, ApJ, 411, 67

Eales S.A., Rawlings S., 1996, ApJ, 460, 68

Eales S., Rawlings S., Law-Green D., Cotter G., Lacy M., 1997, MNRAS, 291, 593

Govoni F., Falomo R., Fasano G., Scarpa R., 1999, A&A, in press (astro-ph/9910469)

Granato G.L., Silva L., Monaco P., Panuzzo P., Salucci P., De Zotti G., Danese L., 2000, MNRAS, in press (astro-ph/9911304)

Fioc M., Rocca-Volmerange B., 1997, A&A, 326, 950

Isobe T., Feigelson E.D., 1990, BAAS, 22, 917

Jarvis M.J., Rawlings S., Willott C.J., Blundell K.M., Eales S., Lacy M., 2000, in, van Breugel W.J., Bunker,A.J., eds, The Hy-Redshift Universe. ASP, in press

Kauffmann G., Haehnault M., 2000, MNRAS, 311, 576

Koski A.T., 1978, ApJ, 223, 56

Lacy M., Kaiser, M.E., Hill G.J., Rawlings S., Leyshon G., 1999a, MNRAS, 308, 1087

Lacy M., Rawlings S., Hill G.J., Bunker A.J., Ridgway S.E., Stern D., 1999b, MNRAS, 308, 1096

Lacy M., Ridgway S.E., Trentham N., 2000, in, Biretta et al., eds, Lifecycles of Radio Sources, New Astronomy Reviews, in press

Laing R.A., Riley J.M., Longair M.S., 1983, MNRAS, 204, 151 (LRL)

Lilly S.J., 1989, ApJ, 340, 77

Magorrian J., Tremaine S., Richstone D., Bender R., Bower G., Dressler A., Faber S.M., Gebhardt K., Green R., Grillmair C., Kormendy J., Lauer T., 1998, AJ, 115, 2285

McCarthy P.J., 1993, ARA&A, 31, 639

McLean I.S., et al., 1993, Proc. SPIE, 1946, 512

McLean I.S., et al., 1994, Proc. SPIE, 2198, 457

McLure R.J., Dunlop J.S., 2000, MNRAS, submitted (astro-ph/9908214)

McLure R.J., Kukula M.J., Dunlop J.S., Baum S.A., Hughes D.H., 1999, MNRAS, 308, 377

Owen F.N., Laing R.A., 1989, MNRAS, 238, 357

Owen F.N., Ledlow M.J., 1994, in, Bicknell G.V., Dopita M.A., Quinn P.J., eds, The First Stromolo Symposium: The Physics of Active Galaxies. ASP Conf. Ser. Vol. 54, p. 319

Pentericci L., 1999, PhD Thesis, University of Leiden

Pentericci L., McCarthy P.J., Röttgering H.J.A., Miley G.K., van Breugel W.J.M., Fosbury R., 2000, ApJ, submitted

Rawlings S., Eales S., Lacy M., 1990, MNRAS, 251, 17P

Rawlings S., Lacy M., Sivia D.S., Eales S.A., 1994, MNRAS, 274, 428

Rawlings S., Blundell K.M., Lacy M., Willott C.J., Eales S., 1998, in, Bremer M.N., Jackson N., Pérez-Fournon I., eds, Cosmology with the New Radio Surveys. Kluwer, Dordrecht, p. 171

Ridgway S.E., Stockton A.N., 1997, AJ, 114, 511

Ridgway S.E., Heckman T., Calzetti D., Lehnert M., 2000, in, Biretta et al., eds, Lifecycles of Radio Galaxies, New Astronomy Reviews, in press

Rigler M.A., Lilly S.J., Stockton A.N., Hammer F., Le Fèvre O., 1992, ApJ, 385, 61

Roche N., Eales S., Rawlings S., 1998, MNRAS, 297, 405

Serjeant S.B.G., Rawlings S., Lacy M., Maddox S.J., Baker J.C., Clements D., Lilje P.B., 1998, MNRAS, 294, 494

Simpson C., Rawlings S., Lacy M., 1999, MNRAS, 306, 828

Stevens R., 1999, DPhil. Thesis, University of Oxford

van Breugel W.J.M., Stanford S.A., Spinrad H., Stern D., Graham J.R., 1998, ApJ, 502, 614

van Breugel W., De Breuck C., Stanford S.A., Stern D., Röttgering H., Miley G., 1999, ApJ, 518, L61

Waddington I., Windhorst R.A., Cohen S.H., Partridge R.B., Spinrad H., Stern D., 1999, ApJ, 526, L77

Willott C.J., Rawlings S., Blundell K.M., Lacy M., 1998, MNRAS, 300, 625

Willott C.J., Rawlings S., Blundell K.M., Lacy M., 1999, MNRAS, 309, 1017

Willott C.J., Rawlings S., Blundell K.M., Lacy M., 2000, in preparation

Willott C.J., Rawlings S., Jarvis M.J., 2000, MNRAS in press (astro-ph/9910422)

Windhorst R., Mathis D.F., Keel W.C., 1992, ApJ, 400, L1

Wold M., Lacy M., Lilje P.B., Serjeant S.B.G., 2000, MNRAS, submitted (astro-ph/9912070)

Zepf S.E., 1997, Nat, 390, 377